Microelectronics Reliability 52 (2012) 2443–2446

Contents lists available at SciVerse ScienceDirect

Microelectronics Reliability

journal homepage: www.elsevier.com/locate/microrel

Power semiconductor module using a bonding film with anisotropic thermal conduction

Yasushi Yamada *

Department of Electrical and Electronic Engineering, School of Engineering, Daido University, 10-3 Takiharu-cho, Minami-ku, Nagoya, Aichi 457-8530, Japan

ARTICLE INFO

Article history:
Received 30 May 2012
Accepted 24 June 2012
Available online 12 August 2012

ABSTRACT

A power semiconductor module using a bonding film with anisotropic thermal conduction has been studied. The bonding film consists of polyamide with a low Young's modulus and *Z*-axis-oriented fine graphite fibers. All the materials of this device, including the insulated substrate and base plate, have low coefficients of thermal expansion. The bonding film is inserted between the baseplate and an aluminum active heatsink. No significant changes in the thermal resistance or cross-sectional microscopy images were found after thermal cycling tests.

1. Introduction

Hybrid and electric vehicles are set to play a vital role in reducing carbon dioxide emissions from automobiles. These vehicles generally use inverters or converters for electrical exchange. Power semiconductor modules (Fig. 1) [1] that consist of many power semiconductor devices are used for these inverters and converters. Power semiconductor devices based on wide band gap materials such as SiC and GaN are promising for next-generation, high-temperature-operation devices [2,3]. However, more advanced packaging technologies are required to operate these devices at high temperatures.

It is essential that power semiconductor modules have high reliabilities for thermal cycling (during which the temperature of the whole device changes), power cycling (which gives local heating resulting in a temperature distribution), and thermal fabrication processes. Of these, the thermal cycle reliability is the most important one to study reliability of the bonding film.

A low thermal cycling reliability is generally caused by a mismatch between the coefficients of thermal expansion (CTE) of semiconductors (e.g., Si, SiC or GaN) and an active heatsink (e.g., Al or Cu). Thus, considerable thermal stresses are generated in packaging during thermal cycling conditions. These stresses are thought to be much greater for elevated temperature operation of wide-band-gap semiconductor devices. Consequently, stress relaxation caused by a CTE mismatch is a critically important issue for next-generation power semiconductor modules.

Several approaches have been proposed to realize stress relaxation, including the use of thermal greases and low-melting-point metals. Thermal greases may cause very low thermal stresses, but they also reduce the thermal conductivity. On the other hand, metals have higher thermal conductivities, but thermal stress is generated during thermal cycling. There is a trade-off relationship between the thermal stress and thermal conductivity of power semiconductor modules. Therefore, some special thermal interface materials have been proposed [4].

In the present study, the thermal cycle reliability of a power semiconductor module with a bonding film that has anisotropic thermal conduction was investigated. The bonding film consists of polyamide, which has a low Young's modulus, and *Z*-axis-oriented thin graphite fibers. The bonding film, structure, and processes of the module are described and thermal characterization, thermal cycle reliability tests, and cross-sectional microscopic observations are performed.

2. Experimental

2.1. Bonding film

Figs. 2 and 3 show cross-sectional and surface views of the bonding film, respectively. The film is approximately 0.1 mm thick. The base material is thermoplastic polyamide. The film contains thin graphite fibers oriented along the *Z*-axis. The volume ratio of graphite is approximately 40% and the Young's modulus in the *Y*-axis (horizontal) direction is quite low, being 0.09 GPa.

When thermal stress is applied to the film, the film may deform along the horizontal plane; this deformation is expected to reduce the thermal stress. The thermal conductivity is highest along the *Z*-axis due to the fine graphite fibers.

Table 1 lists the mechanical properties of the important materials of the power semiconductor module.

* Tel.: +81 52 612 6111; fax: +81 52 612 5623.
E-mail address: yamada-y@daido-it.ac.jp

0026-2714/$ - see front matter © 2012 Elsevier Ltd. All rights reserved.
http://dx.doi.org/10.1016/j.microrel.2012.06.087

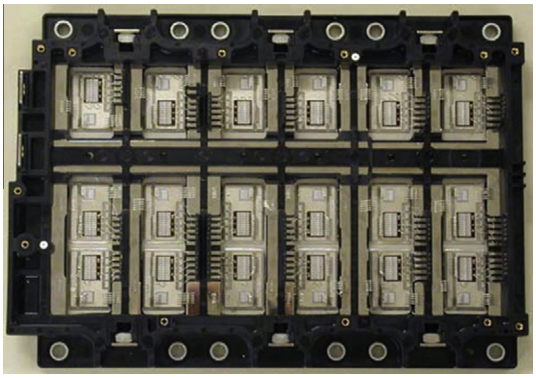

Fig. 1. Power semiconductor module.

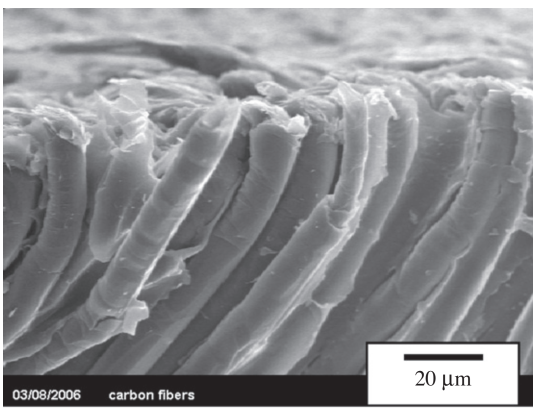

(a) High-magnification image

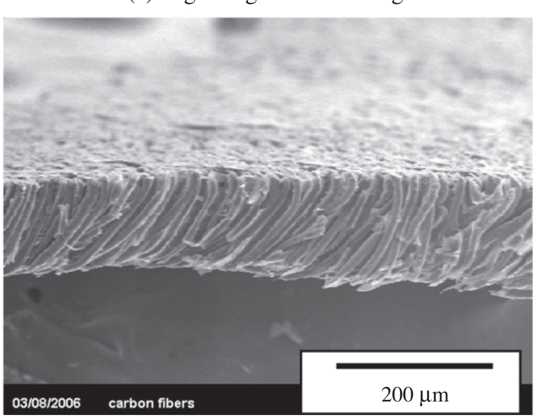

(b) Low-magnification image

Fig. 2. Cross-sectional images of bonding film.

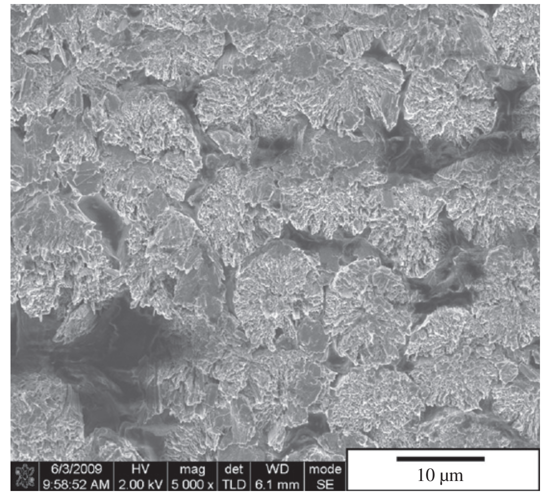

Fig. 3. Surface image of bonding film.

Table 1
Material properties.

Material	Young's modulus (GPa)	Coefficient of thermal expansion (ppm/K)
Si–SiC	400	3
Al alloy	70	23
Bonding film	*X*:0.45, *Y*:0.09	*X*, *Y*:45, *Z*:0
Si	169	3
SiC	450	4
Solder (Sn–3Ag–0.5Cu)	38	21

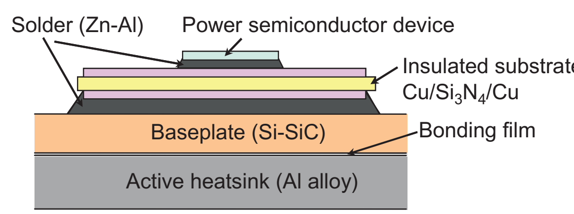

Fig. 4. Structure of power semiconductor module.

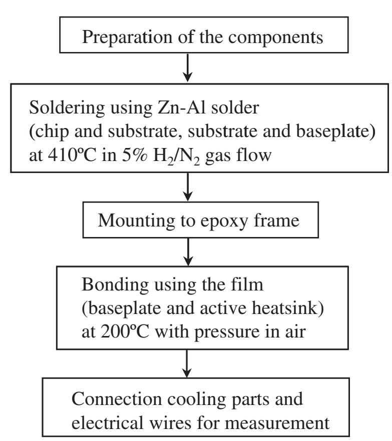

Fig. 5. Module fabrication process.

2.2. Structure of power semiconductor module

The structure of the power semiconductor module with the bonding film is designed by considering the following technical points.

(a) There should be almost no CTE mismatch except around the bonding film. The CTE mismatch around the bonding film is approximately 19 ppm/K.
(b) The power semiconductor device contains joints with high melting points since it is expected to be operated at high temperatures.
(c) No harmful materials, noble metals, or rare metals are used.

Fig. 4 shows the structure of the module. It consists of a power semiconductor device, an insulated substrate such as $Cu/Si_3N_4/Cu$, and a Si–SiC baseplate above the bonding film. The active heatsink

Table 2
Dimensions of components.

Material	Dimensions (mm)	Thermal conductivity (W/mK)
Power semiconductor device	10 × 10 × 0.2	150
Zn–Al solder	10 × 10 × 0.1	110
Cu substrate, Ni plated	15 × 30 × 0.15	400
Si_3N_4 substrate	17 × 32 × 0.3	90
Cu substrate, Ni plated	15 × 30 × 0.15	400
Zn–Al solder	17 × 32 × 0.1	110
Si–SiC baseplate, Ni plated	22 × 40 × 3	200
Bonding film	22 × 40 × 0.1	Refer to Fig. 6
Active heatsink[a]	194 × 85 × 5[b]	140

[a] Between surface and the top of water channel.
[b] Average surface roughness is within 1.6 u.m.

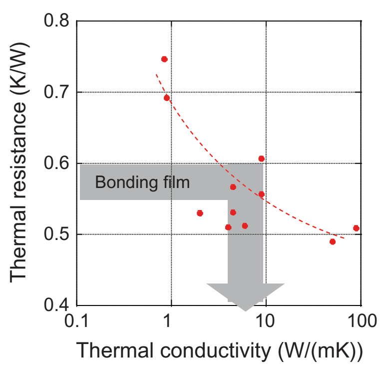

Fig. 6. Relationship between thermal resistance and thermal conductivity (red dots and line are measured results using thermal greases). (For interpretation of the references to color in this figure legend, the reader is referred to the web version of this article.)

is an Al alloy. The bonding film is inserted between the baseplate and the active heatsink. A high-temperature solder such as Zn–Al solder [5–7] is used between the chip and the insulated substrate and between the insulated substrate and the baseplate. The bonding film is joined by heating at 200 °C and applying pressure. The whole fabrication process is shown in Fig. 5 and typical dimensions and thermal conductivities of the components are listed in Table 2.

2.3. Thermal characterization

The *Z*-axis thermal conductivity of the bonding film is characterized by comparing the thermal resistances of the film and commercially available thermal greases. The static thermal resistance is calculated from the measured temperatures of the center of the DC heated chip and the cooling water (measured with an accuracy of 1 K). The temperature and flow rate of the cooling water are kept constant. The thermal grease layer is given a uniform thickness by using small bumps located near the periphery of the thermal flow.

2.4. Reliability examination and analysis

The thermal cycling reliability [8,9] of the fabricated module is examined in air in a thermal cycling chamber. The reliability is evaluated from the thermal resistance between the chip and the cooling water using the method described above. During the thermal cycling test, the module is removed from the test chamber for the thermal measurement and returned after the measurement. After the thermal cycling tests, cross sections of the samples are observed by microscopy.

3. Results and discussion

3.1. Thermal characterization

Fig. 6 shows the thermal resistance between the device and the cooling water. The thermal conductivity of the bonding film is estimated to be more than 5 W/(mK) (which includes the interfacial thermal resistance). The thermal resistance almost saturates at above approximately 10 W/(mK) due to thermal spreading at the baseplate. This makes it difficult to accurately evaluate the thermal conductivity of the bonding film. The thermal properties of the bonding film seem to be approximately similar to those of thermal conductive greases. However the distinction between the bulk and interfacial properties is not clear for the bonding film or thermal greases.

3.2. Thermal cycle reliability

Fig. 7 shows the results of the thermal cycle tests. Thermal resistances between the device and the cooling water remain almost constant up to 1500 cycles in the −40/105 °C test. In addition, there are almost no changes up to 500 cycles in the −40/130 °C test and 200 cycles in the −40/160 °C test with the exception of initial fluctuations.

Fig. 8a and b show cross-sectional images of a sample before and after 1000 cycles of thermal cycle testing at −40/105 °C. Almost no differences are observed; in particular, cracks and delamination are not observed after the test. This suggests that the low Young's modulus of the bonding film reduces the thermal stress generated by the CTE mismatch.

3.3. Discussion of thermal stress

There is almost no CTE mismatch between the chip and the baseplate, whereas there is a large mismatch of almost 19 ppm/K between the base plate and the active heatsink. Although soldering

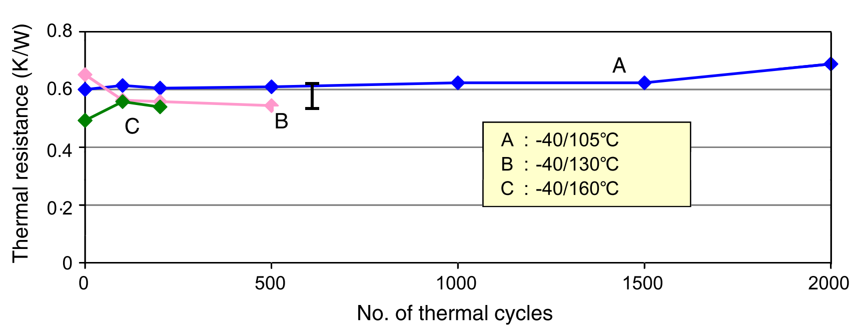

Fig. 7. Thermal resistance change for three thermal cycling test conditions.

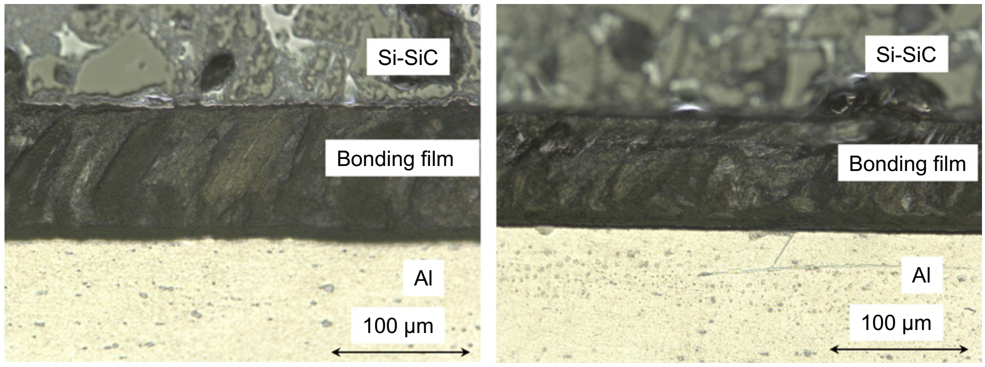

(a) No thermal cycling test

(b) After 1000 cycles of -40/105 °C thermal cycling test

Fig. 8. Cross-sectional image of sample.

generated temperatures above 400 °C, the thermal stress generated during soldering seems to be small due to the small CTE mismatch. On the other hand, a large thermal stress seems to have been generated during the bonding process with the bonding film due to the larger CTE mismatch. Bonding was performed at 200 °C so that some deformation occurs at room temperature or lower temperatures; this deformation seems to be concave down.

The Young's modulus of the bonding film is quite low, being about 0.09 GPa. The film seems to be relaxed or flexed by the concave deformation.

4. Conclusion

Power semiconductor module using a bonding film with anisotropic thermal conduction was studied. A power semiconductor module without harmful materials, noble metals, or rare metals was fabricated. Thermal characterization was performed and thermal cycle reliability was investigated. The proposed structure with the bonding film has promising thermal properties and reliability.

Acknowledgments

The author would like to thank to Tomoe Engineering Co., Ltd. and btechcorp for supporting sample preparation, and also A-Kit CO. Ltd. and Shinwa Co., Ltd. for microscopic observation.

References

[1] Yamada Y et al. Pb-free high temperature solder joint for power semiconductor devices. Trans JIEP 2009;2(1):79–84.
[2] Marcon D et al. GaN-based HEMTs tested under high temperature storage test. Microelectron Reliab 2011;51:1717–20.
[3] Testa A et al. High temperature long term stability of SiC Schottky diodes. Microelectron Reliab 2011;51:1778–82.
[4] Jang K-W et al. A study on thermal cycling (T/C) reliability of anisotropic conductive film (ACF) flip chip assembly for thin chip-on-board (COB) packages. Microelectron Reliab 2012;52:1174–81.
[5] Yamada Y et al. Reliability of wire-bonding and solder joint for high temperature operation of power semiconductor devices. Microelectron Reliab 2007;47:2147–51.
[6] Takaku Y et al. A review of Pb-free high temperature solders for power semiconductor devices: Bi-base composite solder and Zn–Al solder. J ASTM Int 2011;8(1). JAI103042.
[7] Takaku Y et al. Interfacial reaction between Zn–Al-based high-temperature solders and Ni substrate. J Electron Mater 2009;38(1):54–60.
[8] Mermet-Guyenet M et al. Revisiting power cycling test for better life-time prediction in traction. Microelectron Reliab 2007;47:1690–5.
[9] Bouarroudj M et al. Degradation behaviour of 600 V–200 A IGBT modules under power cycling and high temperature environment condition. Microelectron Reliab 2007;47:1719–24.